Diagnosis of the record minimum in Arctic sea ice area during 1990 and associated snow cover extremes

Mark C. Serreze, James A. Maslanik, Jeffrey R. Key, and Raymond F. Kokaly

Cooperative Institute for Research In Environmental Sciences, University of Colorado, Boulder

David A. Robinson

Department of Geography, Rutgers University, Piscataway, New Jersey

Abstract. The Arctic sea ice cover exhibited its record minimum area during 1990, characterized by extensive ice-free conditions during August along the Siberian coast. These reductions are consistent with warm, windy conditions in May and continued warmth in June promoting early melt and reductions in ice concentration, followed in August by strong coastal winds forcing a final breakup and retreat of the pack ice. The unusually warm Arctic conditions in 1990 are part of a larger-scale temperature anomaly pattern, linking the sea ice anomaly to accompanying record minima in Eurasian snow cover.

Introduction

Using the combined passive microwave record from the Nimbus-5 Electrically Scanning Microwave Radiometer and the Nimbus-7 Scanning Multichannel Microwave Radiometer (SMMR), Parkinson and Cavalieri [1989] concluded that no overall trend in Northern Hemisphere ice extent occurred between 1973 and 1987. However, following a reworking of the SMMR record (1978 to 1987), Gloersen and Campbell [1991] demonstrated a small but significant downward trend. Chapman and Walsh [1993], using a longer record (1961 to 1990) based on the weekly US Navy/NOAA National Ice Center (NIC) charts since 1973 (compiled from high-resolution satellite imagery, aircraft and ship reports, but also including passive microwave data when necessary (C. Bertoia, NIC, pers. comm.)), and regional data sources for earlier years, confirm a downward trend. This has been accompanied by upward trends in Northern Hemisphere surface temperatures during the past 30 years over northern Eurasia and northwest North America during winter and spring (with compensating negative trends over southern Greenland and the western subpolar North Atlantic) and reductions in Northern Hemisphere snow extent [Robinson et al., 1993].

As model predictions indicate that the effects of increasing greenhouse gas concentrations will be strongest in the Arctic [e.g., Mitchell et al., 1990], these trends are of interest. Groisman et al. [1994] suggest that the snow cover retreat can be related to an increase in snow cover radiative feedback, accounting for part of the increases in spring temperatures. Within this context, the year 1990 is particularly noteworthy. Based on the Chapman and Walsh [1993] study and our analysis of passive microwave data through 1993, the sea ice area in 1990 is the

smallest yet recorded. Northern Hemisphere snow extent was also at a record low, dominated by record minima over Eurasia from February through September [Robinson et al., 1993]. Finally, Northern Hemisphere temperatures attained record highs for spring, autumn and the annual average [Jones, 1994]. Here, we examine the 1990 sea ice anomaly and argue that its development in part reflects this warming, providing a link with the snow cover extremes.

Observed Ice Conditions

Monthly-mean sea ice areas for 1990 were computed from daily fields of ice concentration derived from Defense Meteorological Satellite Program (DMSP) Special Sensor Microwave/Imager (SSM/I) passive microwave data [Weaver et al., 1987]. We then calculated monthly mean ice areas for 1980 to 1990 by combining the SSM/I (July 1987 onwards) and SMMR (November 1978 to June 1987) records. Both ice data sets were obtained from the National Snow and Ice Data Center and are calculated using the NASA Team Algorithm with global tie points [Steffen et al., 1992]. We define ice area from the number of 25 x 25 km pixels in the entire Northern Hemisphere grid
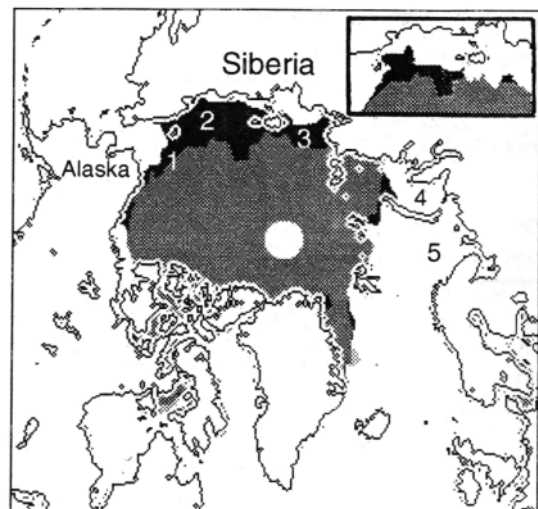
Figure 1. August 1990 ice conditions. Medium shading indicates the 1990 ice area, dark shading areas normally ice covered but ice free in 1990. The inset shows the absolute minimum extent (medium shading) and the area ice free only in 1990 (dark shading). Coastal pixels have been eliminated for clarity. The numbers indicate geographic regions: 1) Chukchi Sea, 2) East Siberian Sea, 3) Laptev Sea, 4) Kara Sea, 5) Barents Sea.

(common to both data sets) having at least a 15% ice concentration. Earlier studies [e.g., Parkinson and Cavalieri, 1989] employed a subset of the grid. Estimates of the 1990 area anomalies were then obtained. The 11-year period was selected as Arctic Ocean temperature data are available for the same years.

Ice areas during May and June 1990 are 6% and 10% below average, respectively. By July, ice area decreases to 16% below normal, largely due to open water along Siberia and in the Barents Sea. The anomaly grows to 21% for August (2.2 x 10^6 km^2 from the mean of 10.5 x 10^6 km^2), almost entirely due to ice-free conditions along Siberia (Figure 1). Essentially no areas in August 1990 show above-average ice cover. These conditions persist into September (19% below normal). Anomalies recalculated after eliminating pixels adjacent to land areas (which may contain false concentration estimates) are similar.

The accuracy of total ice concentrations derived from passive microwave data is generally within 5% in high concentration regions during the cold months [e.g., Steffen and Maslanik, 1988]. However, errors increase to 10 to 15% during summer melt conditions and locally higher due to meltponds and flooded ice. Errors also increase where thin ice is present. Some errors are also expected in our analysis due to different sensor characteristics of SMMR and SSM/I. Although analysis of the SSM/I and SMMR overlap period indicates that the latter problem is minor for our simple analysis of ice area, the effects of summer melt are cause for greater concern. However, ice margins depicted in the SSM/I and NIC analyses show close agreement. Although these are not entirely independent data sets, DMSP shortwave images (0.6 km resolution) for early September 1990 reconfirm the ice margin positions.

As basing the anomalies on the 11-year mean masks large interannual variability in the Siberian sector, we also compiled an absolute minimum field of mean August ice area by treating any pixel with < 15% ice concentration in any year from 1980 to 1990 as open water. We then identified those pixels ice-free only in 1990. This open water area (Figure 1) represents a reduction of 30% in the Siberian sector from 140°E to 160°W north to approximately 80°N. The concentration in this area is 70% averaged over 1980 to 1989 but only 3% in 1990. This difference is too large to be due to errors in the concentration retrievals and further points to the significance of the anomaly.

Atmospheric and Radiative Forcings

The ice anomaly (Figure 1) appears to have its origins in the unusually warm conditions during spring and early summer. To illustrate this link, daily averages of 12-hourly surface temperatures from the International Arctic Buoy Program (IABP) [Colony and Rigor, 1993] were used to compute fields of monthly-mean temperature and the estimated date of snow-melt onset for 1980 to 1990. Results for 1990 were then expressed as anomalies. Following Serreze et al. [1993], melt onset at each grid location was defined as the first day of the first seven-day run of daily mean temperatures of at least 0°C.

The IABP fields are compiled from coastal station data and temperatures measured by drifting buoys. Despite likely positive biases in the buoy temperatures related to insulation by snow cover during winter and radiative heating in summer [Munoz and Martin, 1995], these fields represent the best available Arctic Ocean data source. Employing daily averages reduces these problems. Data errors (< 5% of all data) were flagged through limits checks, with upper and lower temperature bounds varying by month and region, and re-filled through linear interpolation
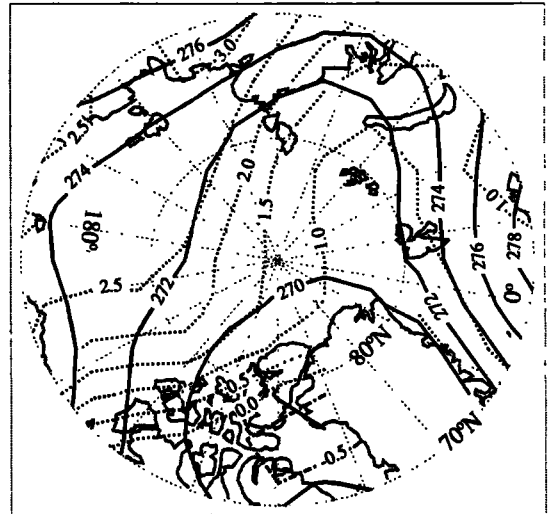

Figure 2. Mean temperature field (solid lines) for May to June 1990 and anomalies (positive: dotted lines; negative: dash-dot lines), both in Kelvins.

between days with good data. We stress that our focus is primarily on the Siberian coast, where the fields are strongly influenced by plentiful station data and few buoys are deployed.

Figure 2 shows the mean temperature and anomaly fields for the two-month period May to June 1990. Positive anomalies are found over all of the Arctic Ocean, with all areas south of an approximate line from the Laptev Sea, across the Arctic Ocean to Alaska showing anomalies between 2.5 to 3.0°C. This pattern is most similar to that for May. During this month, anomalies increase to 5°C along the 180° meridian from 70 to 75°N. June anomalies are largest along the Siberian coast, lying between 2.0 to 3.0°C in the Laptev Sea. Temperatures along the Siberian coast are slightly below and above normal for July and August, respectively (0.5 to 1.0°C). Surface temperature reports from the Historical Arctic Rawinsonde Archive (HARA) [Kahl et al., 1992] confirm these patterns for coastal stations, but with typically larger anomalies. Inferred melt onset is at least ten days
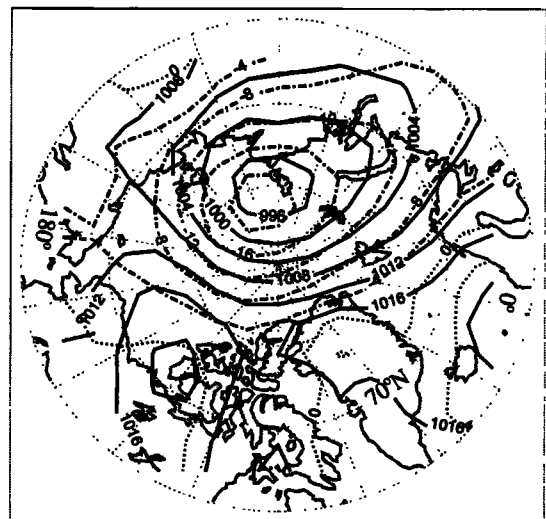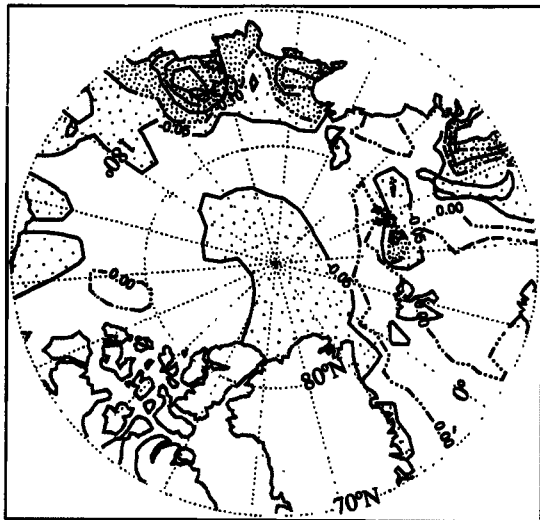

Figure 3. Mean SLP field for May, 1990 (solid lines) and anomalies (positive: dotted lines; negative: dash-dot lines), both in mb.

Figure 4. Surface albedo anomaly field for June 1990. Heavy (light) stippling denotes areas with a negative albedo anomaly of at least 0.10 (0.05).

early along most of the coast from the Laptev Sea eastward to Alaska (late May) and over two weeks early in the northern Laptev Sea (early June), but also early over the remainder of the ice cover. The temperature anomaly fields also argue for rapid melt during June, especially in the Laptev Sea.

The May 1990 mean sea level pressure (SLP) and anomaly field, calculated from National Meteorological Center (NMC) data (1980 to 1990) which include pressure data from the drifting buoys (Figure 3) is highly unusual, dominated by a low of 996 mb (an anomaly of -20 mb) centered at about 80°N, 100°E. As inferred from the isobars, strong southerly winds are found along the coast from the Laptev Sea eastward to north of Alaska. For example, surface winds at station Bukhta Tiski (71.6°N, 128.2°E) average 5.2 m s^{-1} for the month, over twice the 1980 to 1990 mean. Although strong southerly winds are consistent with the temperature anomalies and early melt, they may also explain the local development during this month (as depicted in the NIC and SSM/I analysis) of areas of open water and low concentration ice (20 to 30%) in the Laptev and East Siberian seas.

Schweiger and Key [1994] used the International Satellite Cloud Climatology Project (ISCCP) C2 data set, a compilation of monthly satellite-derived cloud statistics, surface reflectivity, atmospheric temperature, and other variables [Rossow and Schiffer, 1991], to provide a gridded data set of surface broad-band albedo and radiative fluxes for the Arctic Ocean for 1984 to 1990. Although recognizing uncertainties due to problems in cloud/snow discrimination and modeling assumptions, surface albedos for June 1990 along the Laptev and East Siberian sea coasts are shown as 0.10 to 0.30 below the 1984 to 1990 means (Figure 4). Net radiation fluxes are typically 10 to 30 W m^{-2} and locally 50 W m^{-2} above means of 80 to 120 W m^{-2}. The June ISCCP cloud cover north of Siberia is 5 to 15% above normal. As cloud forcing is negative at this time [Schweiger and Key, 1994], this would reduce the surface net radiation. Therefore, the net radiation anomalies reflect the reduced albedo, due both to early melt and expansion of the open-water features first seen in May. Smaller negative albedo anomalies characterize the remainder of the Arctic Ocean. July shows a similar pattern.

As discussed, the ice anomaly continues to grow rapidly during August. Figure 5 shows that the August SLP pattern is dominated by an anomalous anticyclone centered north of Alaska. More typically, the August SLP distribution over this area exhibits a weak closed low [Serreze et al., 1989]. The isobars indicate strong easterly winds over the Chukchi and East Siberian seas, where the ice retreat between July and August was especially pronounced. As observed in the NIC charts, this final retreat was largely accomplished during the third week of August, when the anticyclonic regime was best developed. During summer, the ice motion tends to be to the right of the geostrophic wind, implying a poleward component of the ice motion away from the coast.

Estimated net radiation fluxes for August 1990 along the Siberian coast are > 20 W m^{-2} (30%) above average over an area greater than 4.0 x 10^5 km^2, primarily due to the extensive open water and low concentration ice. Nevertheless, positive anomalies again characterize essentially the entire Arctic Ocean.

Discussion

We conclude that the ice anomaly north of Siberia was set up by unusually warm and windy conditions during May and continued warmth in June, promoting early melt and local breakup of the ice cover, with consequent enhancement of the surface net radiation flux hastening melt through July. Although the anomaly was already large during July, we suspect that the extreme ice-free conditions observed for August may not have developed without the additional circulation "boost" in the form of strong coastal winds, forcing a final breakup and poleward advection of the ice cover.

Other possible contributing factors, such as anomalous ocean heat fluxes, remain to be addressed. It is also not clear why large negative sea ice anomalies did not develop north of Alaska, which experienced a similar wind regime as well as consistently positive temperature anomalies. Perhaps this reflects the particularly early albedo reductions over the Siberian sector (Figure 4). The location of the ice anomaly also contrasts with the general picture provided by Chapman and Walsh [1993] that overall, sea ice reductions have been largest over the Atlantic sector. As suggested from their analysis, this may reflect extensive sea ice over this region during the late 1960s.

As discussed, 1990 also has the smallest snow extent on record for the continental Northern Hemisphere, dominated by rec-

Figure 5. Same as Figure 3, but for August 1990.
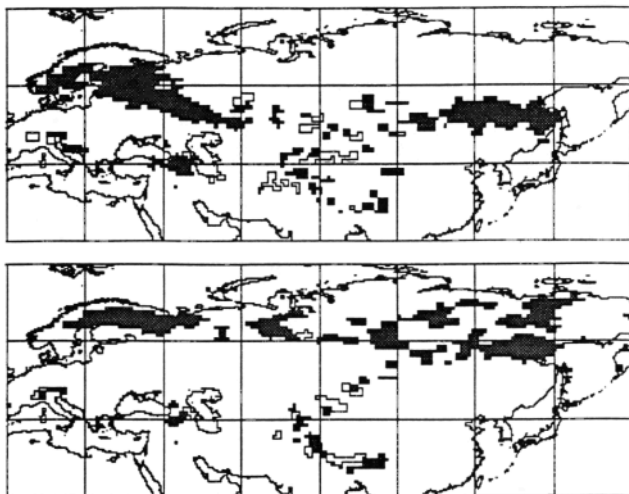
Figure 6. Departures of April (top) and May (bottom) snow cover over Eurasia for 1990. Snow cover in the shaded (open) areas was at least 20% below (above) normal in 1990.

ord minima over Eurasia from February through September (but with the winter 1989/90 average being near normal) [Robinson et al., 1993]. Interestingly, 1990 precipitation over most of the former Soviet Union was exceeded only by two years (1957, 1958) since 1891 [Groisman et al., 1993]. Figure 6 shows the snow cover anomaly field for April and May 1990 with respect to 1980 to 1990 means analyzed from NOAA show charts [see Robinson et al., 1993]. Snow cover is markedly reduced over the western and eastern portions of the continent. The pattern for March is similar. Maps from the Climate Diagnostics Bulletin [NOAA, 1990] for all three months show surface temperatures north of 40°N in the upper 90th percentile of the normal (Gaussian) distribution fit to the 1951 to 1980 base period data for western and eastern Eurasia as well as northwest North America. All regions north of 60°N lie in at least the 70th to 90th percentile, the exceptions being near or slightly below average temperatures over the Canadian Arctic, and in May, over central Eurasia. The IABP data reveal positive temperature anomalies over the Arctic Ocean in May and June, but the April data also reveals large positive anomalies, similar to May.

The unusually warm Arctic Ocean conditions in spring and early summer associated with the sea ice anomaly hence appear to be the high-latitude signal of a much larger-scale temperature anomaly pattern. Although the straightforward interpretation is that the snow cover extremes represent a response to this large-scale forcing, the issue of whether the reduced snow extent itself provided for a feedback accentuating the temperature anomalies [cf. Groisman et al., 1994] merits further investigation.

References

Chapman, W.L. and J.E. Walsh, Recent variations of sea ice and air temperature in high latitudes, *Bull. Amer. Meteorol. Soc.*, 74, 33-47, 1993.

Colony, R.L. and I.G. Rigor, International Arctic Buoy Program Data Report for 1 January 1992-31 December 1992, *Tech. Mem. APL-UW TM 29-93*, APPL, Univ. WA, Seattle, WA, 215 pp, 1993.

Gloersen, P. and W.J. Campbell, Recent variations in Arctic and Antarctic sea-ice covers, *Nature*, 352, 33-36, 1991.

Groisman, P.A., T.R. Karl, R.W. Knight and G.L. Stenchinkov, Changes of snow cover, temperature and radiative heat balance over the Northern Hemisphere, *J. Climate*, 7(11), 1633-1656, 1994.

Groisman, P.A., V.V. Koknaeva, T.A. Belokrylova, and T.R. Karl, Area-average precipitation over the main part of the former USSR, in: *Trends '93. A Compendium of Data on Global Change* (T.A. Boden, D.P Kaiser, R.J. Sepanski and F.W. Stoss, eds.), ONRL/CDIAC-65, Carbon Dioxide Information Analysis Center, Oak Ridge National Laboratory, pp. 906-910, 1993.

Jones, P.D., Hemispheric surface air temperature variations: A reanalysis and an update to 1993, *J. Climate*, 7(11), 1794-1802, 1994.

Kahl, J.D., M.C. Serreze, S. Shiotani, S.M. Skony, and R.C. Schnell, In-situ meteorological sounding archives for Arctic studies, *Bull. Amer. Meteorol. Soc.*, 73(11), 1924-1830, 1992.

Mitchell, J.F.B., S. Manabe, V. Meleshko, and T. Tokioka, Equilibrium climate change and its implications for the future, in: *Climate Change: The IPCC Assessment* (J.T. Houghton, G.J. Jenkins and J.J. Ephraums, eds.), Cambridge University Press, pp. 135-165 plus figures, 1990.

Munoz, E.A. and S. Martin, Gridded Arctic surface temperature data sets: a comparison with Soviet ice station and land temperatures for 1987-88, *J. Climate* (in press).

NOAA, *Climate Diagnostics Bulletin*, March-June 1990, 1990.

Parkinson, C.L. and D.J. Cavalieri, Arctic sea ice 1973-1987: Seasonal, regional and interannual variability, *J. Geophys. Res.*, 94(C10), 14,499-14,523, 1989.

Robinson, D.A., K.F. Dewey, and R.R. Heim, Global snow cover monitoring: an update, *Bull. Amer. Meteorol. Soc.*, 74(9), 1689-1696, 1993.

Rossow, W.B. and R.A. Schiffer, ISCCP cloud data products, *Bull. Amer. Meteorol. Soc.*, 72, 2-20, 1991.

Schweiger, A.J. and J. Key, Arctic Ocean radiation fluxes and cloud forcing based in the ISCCP C2 cloud data set, *J. Appl. Meteorol.*, 33(8), 948-963, 1994.

Serreze, M.C., R.G. Barry, and A.S. McLaren, Seasonal variations in sea ice motion and effects on sea ice concentration in the Canada Basin, *J. Geophys. Res.*, 94(C8), 10,955-10,970, 1989.

Serreze, M.C., J.A. Maslanik, G.R. Scharfen, R.G. Barry, and D.A. Robinson, Interannual variations in snow melt over Arctic sea ice and relationships to atmospheric forcings, *Ann. Glaciol.*, 17, 327-331, 1993.

Steffen, K. and J.A. Maslanik, Comparison of Nimbus 7 Scanning Multichannel Microwave Radiometer radiance and sea ice concentration with Landsat imagery for the North Water area of Baffin Bay, *J. Geophys. Res.*, 93, 10,769-10,781, 1988.

Steffen, K., J. Key, D.J. Cavalieri, J. Comiso, P. Gloersen, K. St. Germain, and I. Rubenstein, The estimation of geophysical parameters using passive microwave algorithms, in: *Microwave Remote Sensing of Sea Ice* (F.D. Carsey, ed.), Geophys. Monogr. Ser., Vol. 68, pp. 201-231, AGU, Washington, D.C., 1992.

Weaver, R., C. Morris and R.G. Barry, Passive microwave data for snow and ice research: planned products from the DMSP SSM/I system, *EOS Trans. Amer. Geophys. Union*, 68(39), 776-777, 1987.

M.C. Serreze, J.A. Maslanik, J.R. Key and Raymond F. Kokaly, CIRES, Campus Box 449, University of Colorado, Boulder, Colorado 80309-0449. (e-mail: serreze@kryos.colorado.edu)

David A. Robinson, Department of Geography, Rutgers University, Piscataway, New Jersey 08854. (email: drobins@gandalf.rutgers.edu)